https://doi.org/10.5194/cp-2022-89
Preprint. Discussion started: 28 November 2022

Climate of the Past Discussions

Patterns of Centennial-to-Millennial Holocene Climate Variation in the North American Mid-Latitudes

Bryan N. Shuman[1]

[1]Department of Geology and Geophysics, University of Wyoming, Laramie, WY, 82071, USA

Correspondence to: Bryan N. Shuman (bshuman@uwyo.edu)

https://doi.org/10.5194/cp-2022-89
Preprint. Discussion started: 28 November 2022

Climate of the Past Discussions

Abstract. Noise in Holocene paleoclimate reconstructions can hamper detection of centennial-to-millennial climate variations and diagnoses of the dynamics involved. This paper uses multiple ensembles of reconstructions to separate signal and noise and determine what, if any, centennial-to-millennial variations influenced North America during the past 7000 yr. To do so, ensembles of temperature and moisture reconstructions were compared across four different spatial scales: continental, regional, sub-regional, and local scales. At each scale, two independent multi-record ensembles were compared to detect any centennial-to-millennial departures from the long Holocene trends, which correlate more than expected from random patterns. In all cases, the potential centennial-to-millennial variations had small magnitudes. However, at least two patterns of centennial-to-millennial variability appear evident. First, large-scale variations included a prominent Mid-Holocene anomaly from 5600-4500 YBP that increased mean effective moisture and produced temperature anomalies of different signs in different regions. The changes steepened the north-south temperature gradient in mid-latitude North America with a pattern similar to the positive mode of the North Atlantic Oscillation (NAO). Second, correlated multi-century (~500 yr) variations produce a distinct spectral signature in temperature and hydroclimate records along the western Atlantic margin. Both patterns differ from random autocorrelated variations but expressed distinct spatiotemporal characteristics consistent with separate controlling dynamics.

https://doi.org/10.5194/cp-2022-89
Preprint. Discussion started: 28 November 2022

Climate of the Past Discussions

1 Introduction

A prominent gap in the conceptual and empirical understanding of the full spectrum of climate variation exists at centennial-to-millennial (cen-mil) scales, particularly for warm climate states (Crucifix et al., 2017; Hernández et al., 2020; Wanner et al., 2008). Cen-mil variations exceed the scales of direct observation and yet are short relative to the resolution of many geological records. The resulting gap in understanding has been recognized for decades (Saltzman, 1982) and continues to thwart efforts to understand 'low-frequency' components of change during the Common Era and other times (Ault et al., 2013). The Holocene Epoch offers a key to this 'missing' scale because cen-mil variability across a broad continuum (Hernández et al., 2020; Huybers and Curry, 2006; Mayewski et al., 2004; Wanner et al., 2008) likely played an important role in shaping ecological, geomorphic, and human history during the past 11,700 years (Fletcher et al., 2013; Shuman et al., 2019; deMenocal, 2001).

Cen-mil variation during the Holocene must have arisen from the interaction among 1) deterministic changes, such as energy balance responses to seasonal insolation trends, 2) chaotic dynamics, such as the fluid behaviors of the atmosphere and oceans and complex biosphere feedbacks, and 3) stochastic events and variability, such as dominates interannual to decadal scales. Non-linear, probabilistic, or transient cen-mil dynamics may have followed the Holocene's orbital and greenhouse gas changes (Claussen et al., 1999; Saltzman, 1982; Wan et al., 2019), autoregressive solar variations (Renssen et al., 2006), and stochastic volcanic eruptions (Kobashi et al., 2017). However, intrinsic, unforced cen-mil variability arising from atmospheric, ocean and sea-ice dynamics may have been equally as significant (Ault et al., 2018). Simulations produce repeated unforced millennial variations, which are similar in magnitude to the effects of early Holocene meltwater forcing and are highly correlated over the northern continents and oceans (Marsicek et al., 2018; Wan et al., 2019). Some variations likely centered on the North Atlantic (Thornalley et al., 2009; Anchukaitis et al., 2019) and the tropical Pacific (Karnauskas et al., 2012) with the potential for far-reaching spatial expressions like those expressed at other time scales. Biosphere feedbacks also may have triggered state shifts against the backdrop of other Holocene variability (Claussen et al., 1999; deMenocal et al., 2000). Externally forced variability may be pronounced at large scales whereas internal variability may generate variations of opposing sign in different regions.

A daunting breadth of variation among individual records matches the wide range of possible drivers (Mayewski et al., 2004; Wanner et al., 2008), but signal-to-noise ratios are small. Analytical or calibration uncertainties of ~2°C (e.g., Russell et al., 2018; Williams and Shuman, 2008; Martínez-Sosa et al., 2021) often dwarf the expected magnitudes of cen-mil temperature variation during the Holocene (~0.5 °C in CCSM3 TRACE simulations; Marsicek et al., 2018; Wan et al., 2019). Slow Earth system components like the ocean can "smooth" the white noise of interannual variability to produce autoregressive variations at cen-mil scales (Huybers and Curry, 2006), but oscillations in many paleoclimate datasets may also be noise generated by other smoothing processes (Fig. 1). Statistical transformations (e.g., curve fitting), sampling effects (e.g., homogenized

https://doi.org/10.5194/cp-2022-89
Preprint. Discussion started: 28 November 2022


Climate of the Past Discussions

samples spanning decades), and a wide range of environmental filtering processes such as sediment mixing, lake residence times, or slow forest turn-over add temporal autocorrelation generating oscillations from white noise via the Slutzky-Yule Effect (Slutzky, 1937). Diagnosing the continuum of weak signals and their complex interactions amid the full array of noise and uncertainties creates a unique challenge for studying cen-mil variability.

The goal of developing a "coherent, falsifiable narrative" (cf. Bender, 2013) may help: what signals are coherent among independent datasets? Are they falsifiably different from null expectations about noise? This paper applies these questions to cen-mil variations during the past 7000 years, after ice sheet influences diminished. The analyses focus on variations previously observed at four spatial scales centered on eastern mid-latitude North America and the western Atlantic to describe the types of Holocene variations expressed in the northern mid-latitudes. Cen-mil variations in this region include long-term dynamics similar to the interannual North Atlantic Oscillation (NAO; Olsen et al., 2012; Orme et al., 2021), correlations among North American droughts and Atlantic temperatures (Shuman et al., 2019; Shuman and Burrell, 2017; Anchukaitis et al., 2019), and possible large-scale temperature variations, consistent in frequency and magnitude with unforced variability simulated by models (Marsicek et al., 2018). To compare the expression of cen-mil variability across spatial scales, dissimilar geographic regions, and different climate variables, the analyses used here focus on a spatial hierarchy of paired multi-record ensembles:

- **Continent-scale cen-mil signals** in both a temperature ensemble derived from European and North American pollen records and an ensemble of North Atlantic records (Marsicek et al., 2018);
- **Regional-scale cen-mil signals** in a networks of temperature and moisture records spanning mid-latitude eastern and central North America (Shuman and Marsicek, 2016);
- **Sub-regional cen-mil signals** in continental and marine temperature reconstructions from two contrasting regions, mid-continent and coastal North America (Shuman and Burrell, 2017; Shuman and Marsicek, 2016); and
- **Site-level cen-mil signals** within the sub-regions, including individual temperature and hydroclimate records (Shuman and Burrell, 2017; Shuman and Marsicek, 2016).

The analyses build upon the detection of cen-mil signals cross-validated across sites and multiple lines of evidence in the northeast U.S. (Shuman et al., 2019), and evidence of different cen-mil signals at the larger regional (Shuman and Marsicek, 2016) and continental scales (Marsicek et al., 2018). To help evaluate potential cen-mil variations, random data series are generated and compared here (Fig. 1). The random series reveal signal characteristics, such as the strength of signal magnitudes and correlations among multi-records ensemble means, which could help distinguish between cen-mil noise and climatically significant variations. To further diagnose the variations, spatial patterns associated with temperature change at 5500-4800 YBP are also evaluated; the interval may include a significant step shift in hemispheric temperatures (Marsicek et al., 2018) and a millennial-scale variation in pollen-inferred temperatures, lake-level changes, and stable isotope records (Shuman and Marsicek, 2016). The mid-Holocene changes may relate to commonly detected anomalies in many North American records and could have characteristics (i.e., changes in the latitudinal temperature gradient over North America) similar to the NAO at

https://doi.org/10.5194/cp-2022-89
Preprint. Discussion started: 28 November 2022

interannual scales (Hurrell et al., 2003; Folland et al., 2009). Together, the results demonstrate a set of cen-mil changes over the past 7000 years, which correlate among ensembles of temperature and moisture reconstructions while differing among regions and scales likely because they represent multiple sets of drivers.

2 Methods

All of the paleoclimate datasets shown here have been previously published. Additional data may help further evaluate the patterns involved, but this paper aims to interrogate and compare the patterns over the past 7000 years in these specific representative datasets to generate an initial evaluation of possible patterns. At the largest ("continental") scale, Marsicek et al. (2018) used 642 fossil pollen records to reconstruct Holocene mean annual temperature (MAT) trends across Europe and North America. They showed cen-mil variations, which correlated across the two continents, between random sub-sets of the reconstructions, and with those detected in an ensemble of geochemical temperature records from the North Atlantic region. The mean European and North American MAT reconstruction and the North Atlantic temperature ensemble are used here as two independent records of possible large-scale cen-mil variations.

At the regional scale, Shuman and Marsicek (2016) synthesized 40 well-resolved paleoclimate records from across mid-latitude eastern North America (ENA). They produced independent reconstructions of 1) the regional mean temperature of the warmest month (MTWM), averaged from 16 pollen-inferred records, and 2) effective moisture, reconstructed using 9 lake-level and 2 dust records averaged as z-scores. The cen-mil variations in the independent MTWM and moisture reconstructions have not been previously compared. To evaluate the spatial patterns involved in the most prominent variation, including whether any spatially coherent patterns exist, the MTWM dataset is also split here into two sub-sets for comparison based on the direction of significant temperature changes previously identified at 5500-4800 YBP (Shuman and Marsicek, 2016). Two ensemble means with uncertainty distributions for each group were produced by randomly selecting and averaging five individual pollen-inferred records; the five records were random were randomly selected out of pool of eight possible records in each directional group with replacement 100 times.

At finer scales, Shuman and Marsicek (2016) also produced sub-regional temperature and moisture reconstructions based on the averages of sub-sets of their records from geographically distinct areas. The resulting mid-continent MTWM reconstruction and the average of the log-transformed dust records are used here to examine cen-mil variation in a continental sub-region. The mid-continent ensemble incorporates 6 pollen-inferred MTWM reconstructions from North Dakota, Minnesota, Iowa, Wisconsin, and Illinois; moisture history was reconstructed from 2 dust records from Minnesota. One centrally located MTWM reconstruction based on fossil pollen data from Sharkey Lake, Minnesota (Camill et al., 2003) is excluded and compared with the sub-regional ensemble to represent the local scale expression of the cen-mil variations.

https://doi.org/10.5194/cp-2022-89
Preprint. Discussion started: 28 November 2022


Climate of the Past Discussions

For a coastal comparison at the sub-regional scale, and to further evaluate cen-mil variation at the finest, local scale in a representative set of individual records, two records from the Atlantic coast are used, which have been identified as having correlated cen-mil temperature and moisture variations (Shuman et al., 2019; Shuman and Burrell, 2017; Shuman and Marsicek, 2016). The alkenone-inferred sea-surface temperature (SST) reconstruction from the Scotian Margin, core OCE326-GGC30 (Sachs, 2007) is used to capture sub-regional temperature variations; its temperature variations correlate with those represented by Shuman and Marsicek (2016)'s regional MTWM reconstruction based on five fossil pollen sites from the northeast U.S. The variations also correlate with those in coastal lake-level reconstructions, such as from New Long Pond, Massachusetts (Newby et al., 2014; Shuman and Burrell, 2017), which is used here to represent the coastal hydroclimate history. Synchrony analyses of the calibrated radiocarbon dates used to constrain the paleoshoreline deposits support the cen-mil details of the lake-level reconstruction by confirming correlations with other near-by sites (Newby et al., 2014). The reconstruction also correlates in detail with pollen-inferred precipitation reconstructions; pollen inferences accurately inform simulations of the stratigraphic record of lake-level changes using forward modelling approaches (Shuman et al., 2019).

1.1 Analyses

To extract the cen-mil component of the eight datasets, curves were fit to the long-term (>6000 yr) trends using loess (locally-weighted scatter plot smoothing) in R (R Core Development Team, 2020) with a smoothing span set to 54.5% (6000 yr/11000 yr) of each data series. An alternative approach using generalized additive mixed models (GAMMs) accounting for temporal autocorrelation in the data did not change the results emphasized here. Because most of the reconstructions represent multi-record ensembles, they have been previously interpolated and binned at 50-yr time steps to combine the unevenly spaced individual data and we apply the same transformation to all of the records here to ensure consistent statistical treatment.

Once detrended, the independent data series for each scale or region were compared using generalized least squares regression (gls in the *mgvc* package in R) to account for correlated errors by assuming a first order moving average structure in the residuals. Pearson's product moment correlation coefficients were also calculated for comparison with null distributions (see below in section 2.2). Additionally, the standard deviation of the detrend temperature series were compared with each other and null distributions to determine potential signal loss. Spectral analyses were performed on the detrended cen-mil residuals using the *multitaper* package in R to compute multitaper spectral estimates (Percival et al., 1993). All of the analyses were applied only to 7000 years of data, although longer segments of the time series are also plotted.

1.2 Null Expectations

The low sign-to-noise ratios and the timescale of cen-mil variation create particular challenges for detecting robust signals. Null expectations can aid detection. To produce distributions of null expectations, 1000 random number series representing 11,000 simulated years with cen-mil variation were generated. For each series, 11,000 numbers were drawn from a normal

https://doi.org/10.5194/cp-2022-89
Preprint. Discussion started: 28 November 2022


Climate of the Past Discussions

155 distribution to produce time series of white noise. Loess curves with a 500-yr span were then fit to each series to generate Slutzky-Yule oscillations by smoothing the random time series to produce temporal autocorrelation characteristics similar to paleoclimatological datasets. Finally, each series was re-sampled randomly 110 times, consistent with the temporal frequency of sub-samples analyzed from many Holocene sediment cores.

160 A second, comparable dataset with a "signal" was generated by selecting one of the random series to serve as a pseudo-signal and averaging it with each of the other 999 individual random series. The result produces a second set of time series that contain 50% signal and 50% random variation, which aim to mimic the noisy appearance of any real cen-mil variations in a set of paleoclimate records; i.e., these time series contain a 'real' shared signal, but it is partially obscured by cen-mil noise.

165 To evaluate relevant characteristics of the random and pseudo-signal time series, sub-sets of six time series were selected at random from each set of 1000 time series and averaged to produce "multi-record" means like the paleoclimate ensembles used here. Pearson's product moment correlation coefficients were calculated comparing the means to all of the 1000 individual series to produce distributions representing random and non-random time series. Additionally, because averaging allows interference among individual series to dampen random variations, standard deviations were also compared. Ensemble means
170 of purely random time series should have low, near-zero standard deviations because random variations from zero cancel each other, but not so with a dataset containing a real signal. The distribution of standard deviation ratios provides a measure of amplitude loss from averaging random versus non-random series.

3 Results

3.1 Characteristics of Simulated Random Variation

175 Simulating random time series and then smoothing over 500-yr windows and re-sampling at intervals consistent with paleoclimatologic records produces time series with cen-mil variation similar to that observed in many Holocene datasets (Fig. 1A, particularly if long trends were added to these series). The random data series include eye catching, but spurious, alignments of variations (e.g., negative correlations in the bottom two series, Fig. 1A) and illustrate two important features that may serve as null expectations for evaluating actual paleoclimate time series. First, averages of multiple records (such as
180 the six shown in Fig. 1A) produce time series with small amplitudes of variation compared to the individual time series because the random fluctuations interfere with each other. The ratio of the standard deviation of the mean time series (bold, Fig. 1A) and that of 1000 individual random series ranges from 0.27-0.41 (median: 0.33). Second, Pearson's correlation coefficients (r) among the random time series center around zero; the 95% distribution of 1000 simulated time series equaled -0.29 to 0.30.

https://doi.org/10.5194/cp-2022-89
Preprint. Discussion started: 28 November 2022

Climate of the Past Discussions
Open Access
EGU

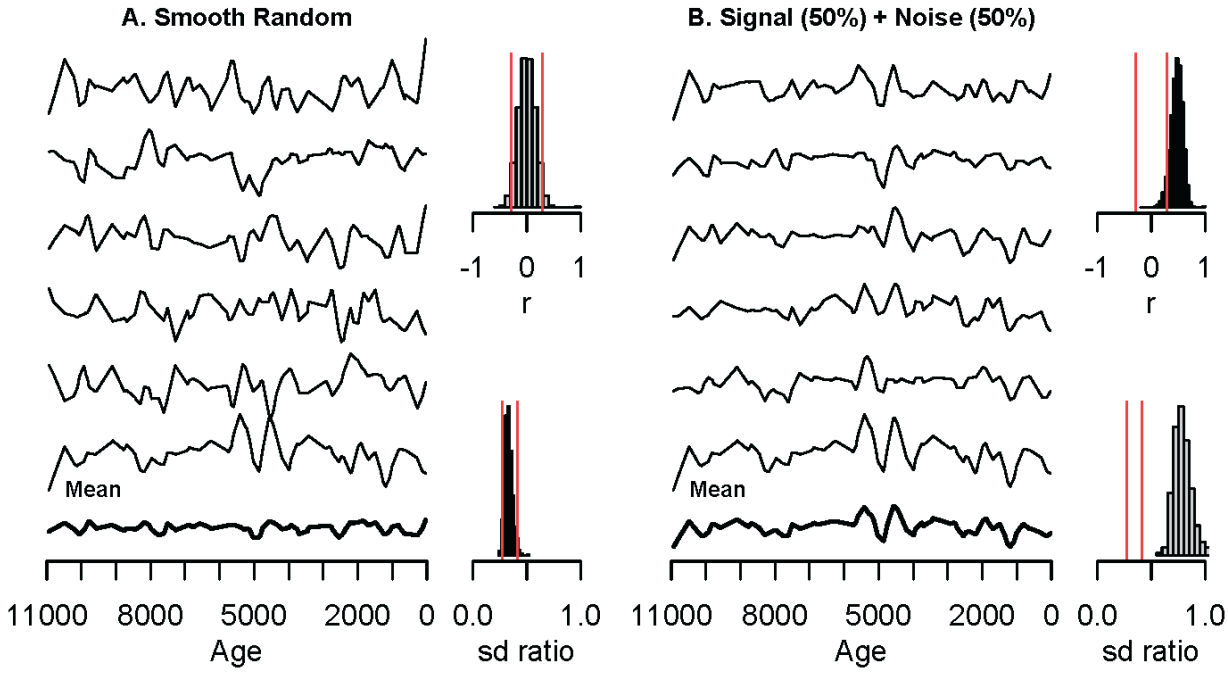

Figure 1 Simulated time series representing A) six white-noise series that have been smoothed to produce spurious oscillations with ~500-yr periods and B) six series as in A, but where the random series has been averaged with a common signal taken from the lower-most series in A. Bold lines at the bottom represent the means of the six series in each case. Histograms show (at the top) the Pearson's product moment correlation coefficients, r, between the means and 1000 similarly generated random (A) or non-random (B) time series, and (at the bottom) the ratio of the standard deviation (sd) of each mean and each of the 1000 simulated series. Red lines show the 95% distributions of the values for the random series.

When a signal is incorporated into the simulated series by averaging the random variations and a common set of fluctuations (Fig. 1B), the results differ from the two null expectations: 1) multi-record means retain a similar amplitude of variation to the individual datasets and 2) most of the correlations among individual time series fall outside the random distribution (>0.30). The six-record mean in Fig. 1B preserves a ratio of standard deviations equal to 0.66-0.97 (median: 0.77) and correlates well (r = 0.96) with the introduced signal (which is the lower-most record in both panels of Fig. 1).

The simulated mean illustrates the potential for averaging ensembles of records to help retrieve weak signals, difficult to discern in individual records. Noise introduced into each of the time series confounded the signals. For example, two event peaks at ca. 5500 and 4500 years in the 'signal' do not appear in all of the series in Fig. 1B, and the absence of one versus the other can create a misleading assessment of a single, asynchronous event depending on the records used. The ensemble mean, however, successfully represents the underlying signal with both peaks (compare the bottom two curves, Fig. 1B).

https://doi.org/10.5194/cp-2022-89
Preprint. Discussion started: 28 November 2022

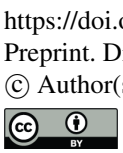

Climate of the Past Discussions
Open Access
EGU

3.2 Long-term Holocene trends

In the actual paleoclimate record from within and around North America, both temperature (red, Fig. 2) and moisture (blue, Fig. 2) express long-term trends, although the trends differ by scale, geographic location, season, and climate variable. The waning presence of the ice sheets and their meltwater effects on Atlantic heat transport drove early Holocene warming of >1.5°C (Dyke, 2004; Shuman and Marsicek, 2016), leading to summer temperature maxima from 8000-5500 YBP. Annual temperatures (MAT) did not peak until after 5500 YBP (Fig. 2A) because of the interacting roles of greenhouse gas and winter insolation forcing, but sea-surface temperatures (SSTs, Fig. 2B) and warm-season temperatures recorded by the mean temperature of the warmest month (MTWM, Fig. 2C) peaked earlier in part because of high summer insolation in the northern mid-latitudes (Berger, 1978). The timing of the summer maximum varied by sub-region (Fig. 2E, G), in part because of the role of added cen-mil variability. Average Atlantic temperatures (gray, Fig. 2B) show a distinct long-term pattern because of large anomalous Holocene cooling trends in records from the western Atlantic (Marsicek et al., 2018; Sachs, 2007), which produce a contrast with other datasets and simulations known as the "Holocene Temperature Conundrum" (Liu et al., 2014).

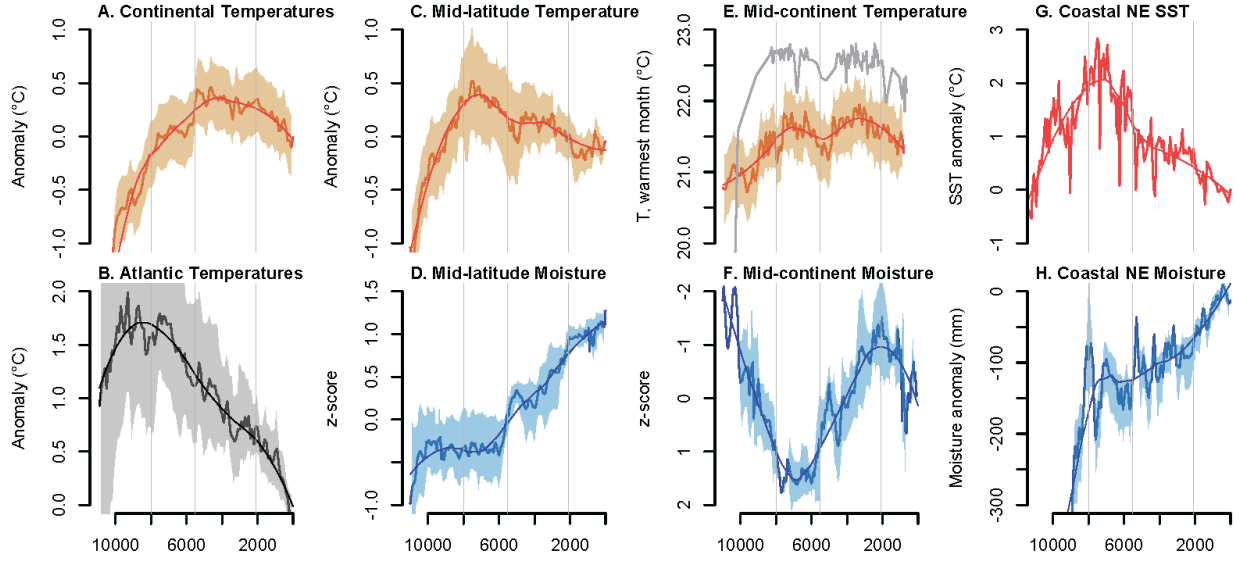

Figure 2 Holocene paleoclimate time series spanning from continental to local scales representing A) Europe and North America mean annual temperatures (MAT)(Marsicek et al., 2018), B) North Atlantic temperatures (Marcott et al., 2013; Marsicek et al., 2018), C) mid-latitude North American mean temperatures of the warmest month (MTWM)(Shuman and Marsicek, 2016), D) mid-latitude ENA hydroclimate indicated by lake-level and dust records (Shuman and Marsicek, 2016), E) mid-continent North American MTWM records (Shuman and Marsicek, 2016), F) mid-continent North America hydroclimate (dust) records (Dean, 1997; Nelson and Hu, 2008; Shuman and Marsicek, 2016), G) alkenone-inferred SST from the Scotian Margin, core OCE326-GGC30 (Sachs, 2007; detrended as in Shuman and Marsicek, 2016), and H) effective precipitation estimated from the lake-level history of New Long Pond, Massachusetts (Newby et al., 2014). In E, the individual MTWM reconstruction from Sharkey Lake, Minnesota is shown (black line) for comparison with a sub-regional average, which excludes the Sharkey Lake record. Vertical lines denote 8000, 5500, and 2100 YBP. Loess fits used to detrend the records in Fig. 3 are shown.

https://doi.org/10.5194/cp-2022-89
Preprint. Discussion started: 28 November 2022


Climate of the Past Discussions

Moisture availability also includes long trends with most areas experiencing higher effective moisture in the late-Holocene than at other times (Fig. 2D, F, H). The mid-Holocene was dry in most areas, but the influence of the Laurentide Ice Sheet before ca. 8000 YBP enhanced moisture availability in the mid-continent (Fig. 2F) and suppressed it substantially along the eastern coast (Fig. 2H)(Shuman and Marsicek, 2016). As a result of the opposing directions of regional change, the average moisture available across all of mid-latitude ENA remained intermediate until after 5500 YBP when it rose sharply toward present (Fig. 2D). Cen-mil variation modified these trends in different ways in different areas.

3.3 Patterns of Cen-Mil Variation

Cen-mil variations rarely departed significantly from the long trends with respect to reconstruction uncertainties in the eight time-series examined here (Fig. 2); detrended series remain near-zero throughout the Holocene (Fig. 3). Detrended temperatures vary only 0.25-0.5°C, which is consistent with Common Era fluctuations (PAGES 2k Consortium, 2013). The rarity of significant anomalies affirms the weak signal-to-noise ratio at cen-mil scales.

Several notable exceptions are apparent, however. A mid-Holocene wet phase from 5600-4500 YBP is the most prominent anomaly. It departs significantly from the mean trends in the ENA mid-latitude, mid-continent, and northeastern coastal moisture reconstructions (Fig. 3B-D). Along the northeast coast, the duration only extends from 5500-5000 YBP (Newby et al., 2014). Additional multi-century departures appear at 7800-7600 and 900-700 YBP in the mid-continent moisture ensemble (Fig. 3C) and 8200-7700, 7700-7200 (negative), 4400-4200, and 3400-3100 YBP in the northeast coast (Fig. 3D). (Note that the features recorded in the northeast coast have been replicated in multiple reconstructions; they are not specific to the site or method, Shuman et al., 2019, and are confirmed by detailed radiocarbon dating across multiple cores and sites, Newby et al., 2014, Shuman and Burrell, 2017).

Given the small magnitude of most cen-mil variations, correlations and the consistency of signal strength among independent datasets provide important additional support for the rigor of the signals. For example, the Pearson's product-moment correlation between the cen-mil features of the continental and Atlantic temperature records equals 0.41 (95% range: 0.20-0.60), which is outside the range of random expectations (Fig. 3A). The slope of the generalized least-squares model relating the two series differs significantly from zero (0.46±0.17) and the ratio of their standard deviations (0.94-1.1) indicates similar signal magnitudes (Fig. 3A).

The strongest correlation among two independent time series of cen-mil residuals comes from the ENA mid-latitude scale (Fig. 3B). One time series representing this scale derives from fossil pollen (MTWM, Fig. 3B) and the other from sedimentary evidence of lake-level and dust deposition changes (moisture z-scores, Fig. 3B). Despite the different methods involved, both

https://doi.org/10.5194/cp-2022-89
Preprint. Discussion started: 28 November 2022

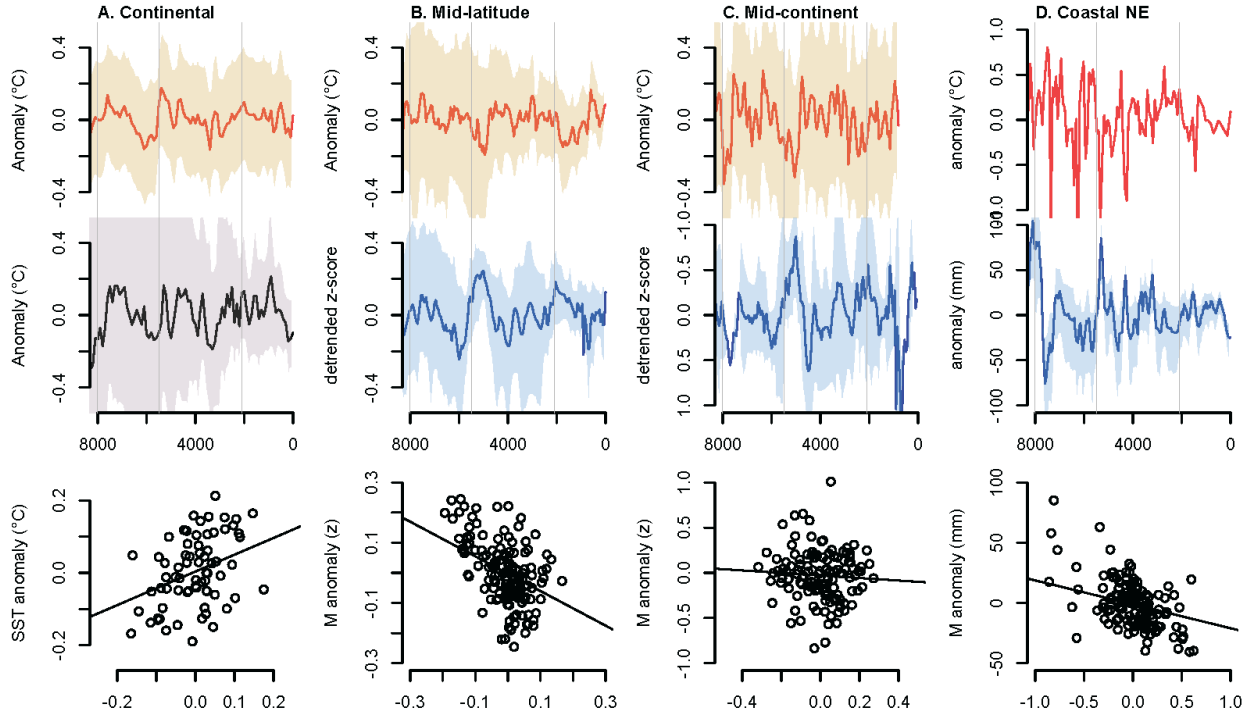

Figure 3. The same paleoclimate time series as in Fig. 2 are shown after detrending. Vertical lines in the upper panels mark 8000, 5500, and 2100 YBP. Scatter plots show the correlations of each pair of cen-mil residuals for each scale or region over the past 7000 years. Lines in the scatter plots represent generalized least-squares models, which account for temporal autocorrelation. "M" indicates moisture on the y-axes and "T", temperature, on the x-axes of the scatter plots.

mid-latitude datasets represent the same region and have large, if not significant, departures from the mean trends at 5600-4500 and 2100-750 YBP (as well as 10,700-9200 YBP apparent in Fig. 2B). Brief departures of the opposite sign appear centered at 750 YBP in both series (Fig. 3B). Pearson's product-moment correlation between the two ensembles equals -0.50 (95% range: -0.37 to -0.62), and the slope of the generalized least-squares model differs significantly from zero (0.57±0.11)(Fig. 3B). Cooling coincides with moistening at this scale.

At the scale of the mid-continent sub-region, the cen-mil correlation between temperature and moisture is weakest (Fig. 3C). Both ensembles record a large departure from the long-term trends at 7800-7600 and 5600-4500 YBP, but the sign of the correlation differs between the two events. The other features of the residual series are not correlated. Neither the Pearson's product-moment correlation coefficient (r = -0.07, 95% range: -0.24 to 0.11) nor the slope of the generalized least-squares model (-0.14±0.22) differ significantly from zero (Fig. 3C).

https://doi.org/10.5194/cp-2022-89
Preprint. Discussion started: 28 November 2022


Climate of the Past Discussions

In the coastal northeast sub-region, however, the cen-mil variation in the SST and lake-level records correlates significantly (Fig. 3D)(Shuman and Burrell, 2017). Both include repeated multi-century cool and wet fluctuations, particularly at 5500-5000, 4400-4200, 3400-3100, 2100-1300, and 1200-0 YBP. These events alternate with warm and dry departures from the long trend at 4900-4600, 4200-3900, 2900-2100, and 1300-1200 YBP (Newby et al., 2014; Shuman and Marsicek, 2016). The Pearson's product-moment correlation coefficient ($r = -0.44$, 95% range: -0.56 to -0.29) and the slope of the generalized least-squares model (-19.8±5.0) both differ significantly from zero (Fig. 3D). Similar relationships exist with pollen-inferred MTWM for the coastal region (Shuman and Marsicek, 2016).

Correlations outside the range of simulated random time series ($r > 0.3$) mark the pairs of independent data for each scale ($r > 0.44$), except regionally in the mid-continent, but they also include correlations between several other independent datasets (Fig. 4):

- The continental pollen-inferred MAT reconstruction correlates with the moisture ensembles from mid-latitude ENA ($r = 0.60$, 95% range: 0.48 to 0.70) and the northeast U.S. coastal ($r = 0.38$, 95% range: 0.23 to 0.51);
- The pollen-inferred MTWM for mid-latitude ENA correlates with the moisture ensembles from the mid-continent ($r = 0.43$, 95% range: 0.28 to 0.56) and from the northeast coast ($r = -0.34$, 95% range: -0.19 to -0.48).

Consistent with different sign anomalies in different regions, the strong correlation between the continental-scale MAT reconstruction and the mid-latitude (ENA M) moisture ensemble (Fig. 4) is notably positive despite a negative temperature-moisture relationship within mid-latitude ENA (ENA T versus ENA M in Fig. 3B, see also Fig. 4). Other similar magnitude correlations also exist (Fig. 4), but they involve pairs of sub-regional subsets of the larger mid-latitude ensembles and are not wholly independent. Overall, the ENA mid-latitude reconstructions correlate best with each other and the greatest number of other reconstructions.

https://doi.org/10.5194/cp-2022-89
Preprint. Discussion started: 28 November 2022

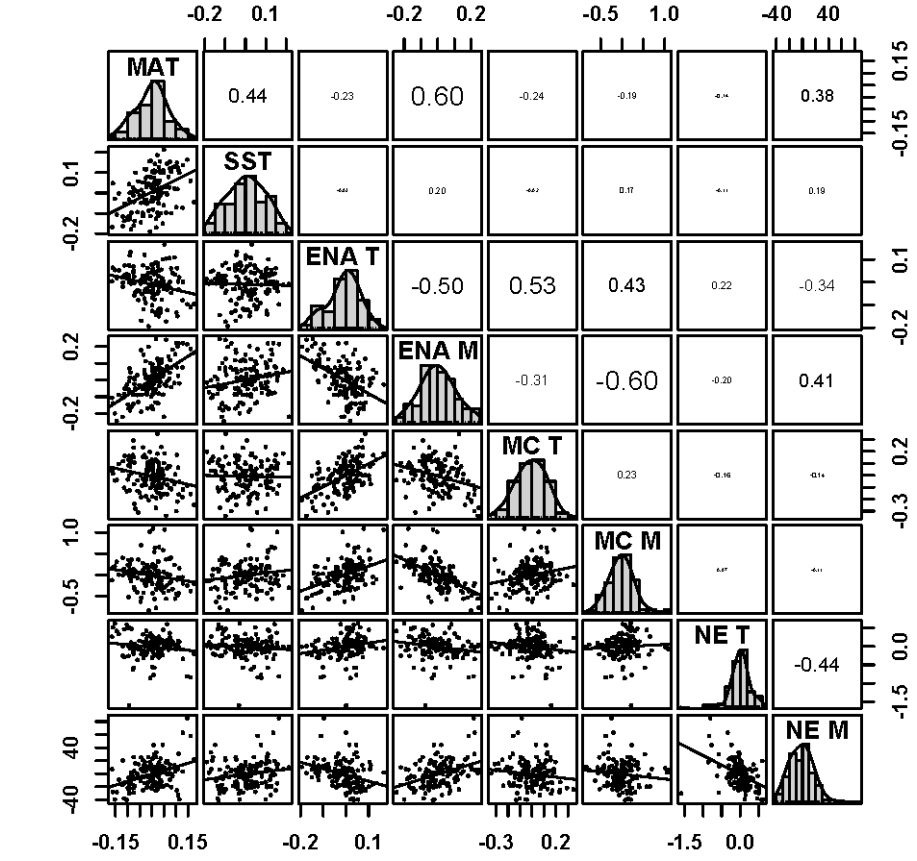

Figure 4. Scatter plots represent the relationships among all detrended time series in Fig. 3 labelled along the diagonal by region: MAT for continental-scale mean annual temperatures; SST, Atlantic temperatures; ENA, eastern North American mid-latitudes; MC, mid-continent North America; NE, northeast coastal sites; T, mean temperatures of the warmest months; M, effective moisture. Lines represent linear fits. Histograms show the distribution of each detrended variable. Correlation coefficients in panels at the upper right are scaled by the strength of the correlation.

The absence of correlations among some scales, regions, and variables is also important. For example, the northeastern coastal records correlate with each other, but only weakly with any other regions or scales. The composite of Atlantic temperature records at the largest scale also does not correlate with other reconstructions except the pollen-inferred MAT record from the same scale (Fig. 4).

3.4 Spectral analyses

Multitaper spectral analyses of the detrended time series (Fig. 3) show that maximum spectral power exists at the scale of multiple millennia for most of the scales, regions, and variables (Fig. 5). The continental-scale spectra based on pollen and

https://doi.org/10.5194/cp-2022-89
Preprint. Discussion started: 28 November 2022

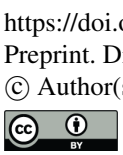

Climate of the Past Discussions
Open Access
EGU

315 marine records indicates increasing power from 500 to 2000 yr periods with a modest minimum at 1200-1500 yr periods. The series representing the ENA mid-latitude region agree with each other and include substantially more power than at larger spatial scales at 2000 yr (4000-1500 yr) periods. The mid-continent sub-regional series agree less well with each other than the others, but also contain increasing spectral power as periods extend to 2000-4000 yr periods.

320

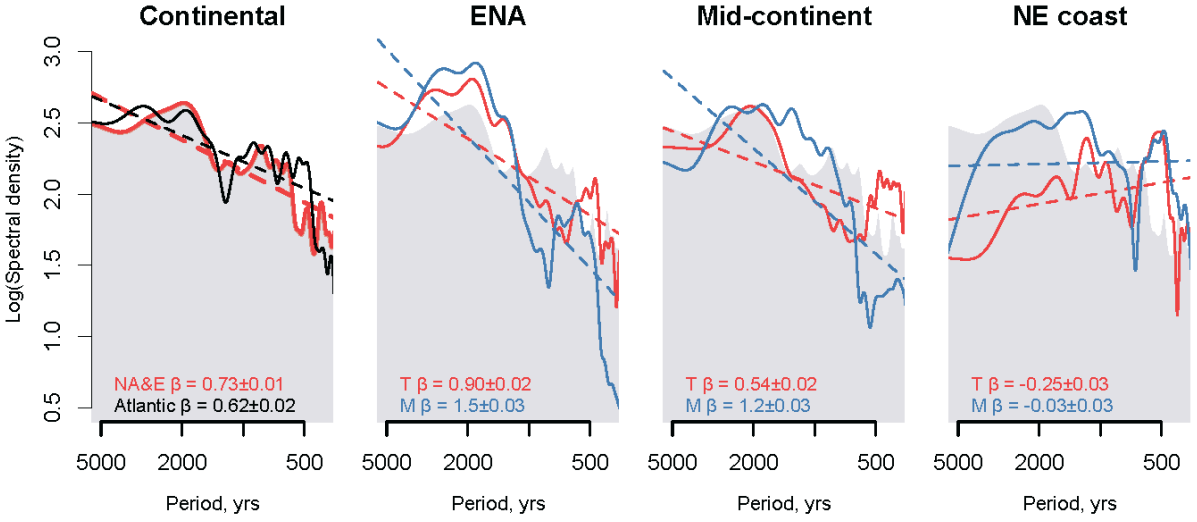

Figure 5. Multitaper spectral density plots show each time series of detrended cen-mil residuals in Fig. 3 with respect to log spectral power and period. Beta values represent the slope of linear fits in log(density)/yr. Gray shading represent the spectrum of the pollen-inferred MAT from Europe and North America (NA&E) for comparison. Red curves represent temperature (T) time series and 325 **blue curves, moisture (M).**

The spectra from the northeast coastal region differ most significantly from the others (Fig. 5). They both contain peaks in power at 500-yr periods, which the other series lack. They also show substantially less power at multi-millennial scales, creating the absence of an increase in power with period length. Thus, the coastal region expresses a higher frequency of 330 variability in the cen-mil bands than the continental areas and larger spatial scales considered here.

3.5 Mid-Holocene changes with north-south differences

The differences across spatial scales and regions (Fig. 3) raise the question of the spatial patterns involved. The full ensemble of MTWM reconstructions from mid-latitude ENA (Shuman and Marsicek, 2016) enables further evaluation the most prominent cen-mil feature of the different ensembles, which is the significant mid-Holocene anomaly from ca. 5600-4500 YBP 335 (Fig. 3). To aid the analysis of this anomaly, the MTWM ensemble can be sub-divided according to records that warmed versus cooled based on subtracting the reconstructed temperature from when the anomalies were well developed (4800 YBP) from the temperatures near the beginning of the event (5500 YBP, Fig. 6). Doing so identifies a set of generally southern records,

https://doi.org/10.5194/cp-2022-89
Preprint. Discussion started: 28 November 2022

Climate of the Past Discussions

regardless of longitude, which warmed from 5500 to 4800 YBP, and a northern tier of sites that cooled; when any two near-by north and south sites are paired across most longitudes, the southern site warmed rapidly from 5500 to 4800 YBP, while the northern site cooled (Fig. 6B). In the northeast U.S., a deviation from the north-south pattern produces a strong coastal-inland contrast of coastal cooling versus inland warming (Marsicek et al., 2013)(Fig. 6B). Together the spatial distribution of MTWM changes bear resemblance to the historic (1948-2015 CE) correlation between June-July-August temperatures and the North Atlantic Oscillation index, including a band of minimal changes through the center of the region (Fig. 6B).

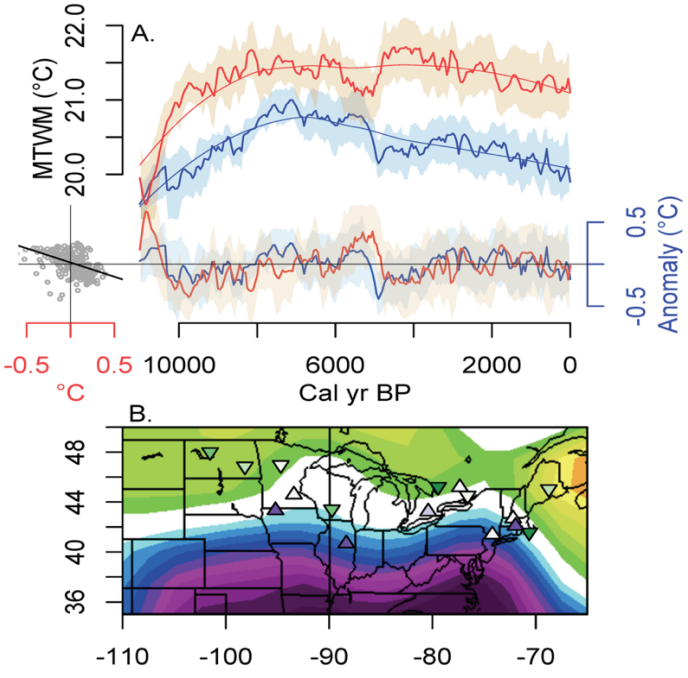

Figure 6. A) The average time series of mean temperature of the warmest month (MTWM) from sites that either warmed from 5500-4800 YBP after a cool millennium (red) or cooled after a warm period (blue) are shown with loess fits with a 6000-yr span and, below, after the loess trend has been subtracted; the red detrended curve for southern sites is shown inverted for comparison. The inset scatter plot compares the two detrended series with the southern-site MTWM anomaly on the x-axis (red) and the northern-site MTWM anomaly on the same y-axis as the detrended time series (blue). The 50% range of 100 possible 5-site averages is shown as the shaded uncertainty for each series. B) Mapped triangles show the locations of warming (upward triangles) and cooling (downward triangles). Green shading reflects the magnitude of cooling; purple, the magnitude of warming. Underlying contours indicate historic (1948-2015 CE) correlations between June-August mean temperatures and the North Atlantic Oscillation index from https://www.psl.noaa.gov/data/correlation/; shades of green show positive and purple negative correlations up to 0.4.

The contrast between northern (blue curve, Fig. 6A) and southern sites (red curve, Fig. 6A) represents changes in the steepness of the north-south summer temperature gradient (the difference between the curves). The northern sites (blue curve, Fig. 6A) track a long-term pattern of warming before 8000 YBP, interrupted by evidence of the 8200 YBP cool event. Subsequent cooling accelerated at ca. 5000 YBP until a warm phase from 4800-3000 YBP interrupted the cooling, which resumed after

https://doi.org/10.5194/cp-2022-89
Preprint. Discussion started: 28 November 2022

Climate of the Past Discussions
Open Access
EGU

2000 YBP. At the southern sites (red curve, Fig. 6A), early Holocene warming occurred early and rapidly, and temperatures remained high until after 4000 YBP. A mid-Holocene phase of low temperatures punctuated the warm phase and was terminated by rapid warming at 5000 YBP, which yielded maximum temperatures from 4800-3900 YBP.

The detrended cen-mil residuals from the independent northern and southern mean time series correlate negatively (r = -0.36, 95% range: -0.47 to -0.24). Both series have phases marking distinct, anti-phased departures from the long-term trends, which do not differ significantly from each other except in sign (Fig. 6A, note that the detrended MTWM series for the southern sites is inverted for comparison). The northern and southern MTWM means have standard deviations of 0.13 and 0.20°C respectively after detrending; the ratio equals 0.63, which is outside the 95% range of randomly simulated series (Fig. 1A). The slope of the generalized-least squares model comparing the two sets of residuals equals -0.37±0.10 (inset scatter plot, Fig. 6A).

The regional MTWM means shifted most prominently at ca. 10,000 and 5000 YBP and increased the temperature difference between the northern and southern tiers of sites. Changes at ca. 8000 and 3900 YBP acted to relax the temperature difference. The patterns are robust to excluding sites with the largest inferred changes (Fig. 7), such as Lake West Okoboji, Iowa, and Chatsworth Bog, Illinois, the sites with the greatest warming at ca. 5000 YBP (Fig. 6B). The changes also extend beyond any specific pollen assemblages, occurring from areas of prairie to eastern deciduous forests (Fig. 6B).

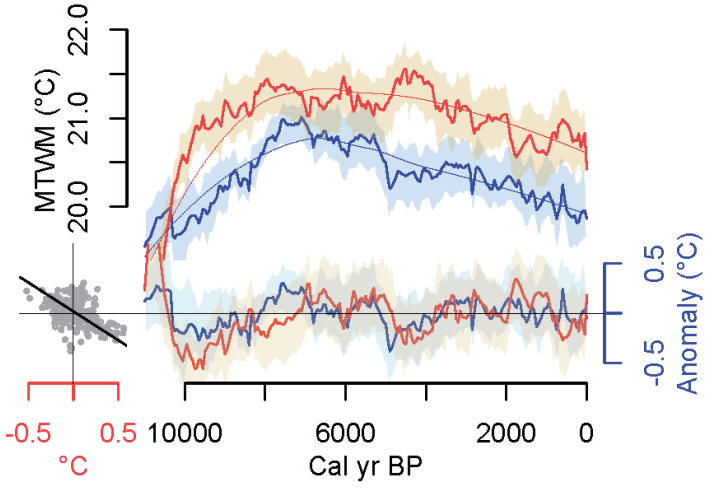

Figure 7. Same as in Fig. 6A except with MTWM reconstructions from Lake West Okoboji, Iowa, and Chatsworth Bog, Illinois, excluded. The records represent the two sites, marked by dark purple triangles in Fig. 6B, with the greatest warming from 5500-4800 YBP.

https://doi.org/10.5194/cp-2022-89
Preprint. Discussion started: 28 November 2022


Climate of the Past Discussions

4 Discussion

4.1 Patterns of cen-mil variability

In Holocene temperature reconstructions spanning a range of scales from multiple continents to individual sites, a few patterns of cen-mil variation appear evidence within the past 7000 years, after dynamics related to ice sheets and meltwater were no longer significant (Fig. 3). The temperature variations were small (<0.25°C), which challenges detection using most standard techniques and indicates that they may not be robust to all methodological decisions for reconstructing them (Williams and Shuman, 2008). For example, pollen-based reconstructions may require high taxonomic resolution with regional differentiation among morphotypes as well as rejecting insignificant reconstructions from individual sites (Marsicek et al., 2018; Telford and Birks, 2011). However, some variations correlate well with independent datasets generated using different approaches and retain signal amplitude after multiple records have been averaged (Fig. 4). The consistency is greater than expected from random autoregressive variations (Fig. 1) and highlights two prominent patterns of cen-mil variation.

First, at the broadest scale, the continental-scale MAT (top, Fig. 3A), mid-latitude MTWM (top, Fig. 3B) and mid-latitude hydroclimate reconstructions (bottom, Fig. 3B), and, to a lesser degree, average Atlantic temperatures (bottom, Fig. 3A) share a correlated pattern of multi-millennial variation (Fig. 3-4) with spectral power centered at periods around 2000 years (Fig. 5). Broad spectral peaks confirm that the variations are not cyclical but include maxima in continental-scale MAT at 5500 and 2100 YBP (vertical lines, Fig. 3). Minima occur at 6000 and 4000 YBP and a rapid shift marks the onset of the most significant anomaly from 5600-4500 YBP. The pattern follows the opposite sign with cooling at 5500 and 2100 YBP in ENA and mid-continent MTWM records (Fig. 3B-C) and propagates down to the scale of individual mid-continent sites such as Sharkey Lake, Minnesota (black line, top, Fig. 2E). Mean mid-latitude moisture availability in ENA also has these features with high moisture levels beginning at 5500 and 2100 YBP (blue, Fig. 3B). At least some of the temperature variations are expressed as the north-south anti-phased pattern across mid-latitude ENA (Fig. 6-7), which bears some similarities to the summer North Atlantic Oscillation at interannual time scales (Fig. 6B). The pattern also bears similarities to those detected during the Younger Dryas in ENA (Fastovich et al., 2020). The correlations among temperatures and moisture at cen-mil scales (Fig. 3-4) differ from the relationships represented by the long Holocene trends (Fig. 2), indicating that different processes were likely involved.

Second, 500-yr variability appears superimposed on the broad-scale variations along the northeast coast (Fig. 3-5). The northeastern SST reconstruction correlates with the drought history along the coast (Fig. 3D), but the high frequency (multi-century) variations appear absent in most other regions (Fig. 5). The northeast regional records lack strong correlations to other areas or scales (Fig. 4). The large-scale Atlantic temperature composite also lacks this variability (Fig. 5), which may be muted if different portions of the Atlantic have different sign fluctuations (Shuman et al., 2019). Within the network of northeastern lake-level records, the spatial patterns of the two patterns of cen-mil variation differ and may confirm two superimposed dynamics: the widely prominent event from 5500-5000 YBP includes a strong inland-coastal contrast, but repeated warm-dry

https://doi.org/10.5194/cp-2022-89
Preprint. Discussion started: 28 November 2022


Climate of the Past Discussions

events at 4900-4600, 4200-3900, 2900-2100, and 1300-1200 YBP, which drive the spectral peak at 500 years (Fig. 5), do not (Newby et al., 2014; Shuman and Burrell, 2017).

The first pattern may be stronger at regional scales across mid-latitude ENA than across the larger continental-to-hemisphere scale represented by the MAT reconstruction (Fig. 3-4) because related variations of different sign cancel at the largest scales. The continental MAT and Atlantic temperatures include many records in the eastern Atlantic and European regions, which may include different influences and expressions. The mid-latitude ENA reconstructions, instead, may emphasize variations common at the scale of westerly waves or other synoptic features. Sub-regional subsets whether they represent continental versus coastal areas (Fig. 3C-D) or northern versus southern areas (Fig. 6-7) highlight added regional differences.

In mid-continent North America, cen-mil variation appears weaker and less consistent than in other areas (Fig. 3-4). Potential teleconnections and interactions in this region may be more variable than in other areas, such as the northeast coast. The difference is analogous to different teleconnected responses to tropical Pacific and North Atlantic variability today, which have more consistent responses to interannual variability in some areas than others.

4.2 Mid-Holocene Anomaly

The most significant anomaly in many records falls between 5600-4500 YBP (Fig. 2-3, 6-7). Qualitative evidence of a "Mid-Holocene Anomaly" has existed for decades in North America. At Elk Lake, Minnesota, the varve record there contains a phase of reduced dust deposition and varve thicknesses (Dean, 1997). Fossil pollen records from the Great Plains, such as Creel Bay, Spiritwood, and Moon lakes, North Dakota, and Pickerel Lake, South Dakota, contain a conspicuous interval of low *Ambrosia* (ragweed) pollen (Grimm, 2001). A prominent paleosol (BS3 at the Wauneta Roadcut) interrupts the Bignell Loess of western Nebraska at this time (Miao et al., 2007). Lake-level records in the Rocky Mountains indicate a distinct phase of high water in Wyoming and Colorado (Shuman et al., 2014; Shuman and Marsicek, 2016), while those in inland areas of the northeast U.S. record low water at the same time (Newby et al., 2011; Shuman and Burrell, 2017). Submerged tree stumps within Lake Tahoe, California, date to this interval (Benson et al., 2002), which also includes evidence of simultaneous anomalies in other regions (Magny et al., 2006; Magny and Haas, 2004), such as the Mediterranean Sea (Alboran Cooling Event 2; Cacho et al., 2001; Fletcher et al., 2013) and Africa (Berke et al., 2012; Thompson et al., 2002).

A similar mid-Holocene anomaly has been widely recognized across the North Atlantic region. Records document shifts in deep water from 5500-4700 YBP (Oppo et al., 2003) and other distinct anomalies from the Labrador to Norway in sea-surface temperatures, salinity, loess and precipitation (Giraudeau et al., 2010; Jackson et al., 2005; Larsen et al., 2012; Orme et al., 2021). Likewise, an inferred positive phase of the North Atlantic Oscillation (Olsen et al., 2012) coincides with distinct and contrasting phases of anomalous warmth on the Labrador Shelf from 5700-4800 YBP (Lochte et al., 2020) and cold in the Florida Strait from 5500-4400 YBP (Schmidt et al., 2012). An earlier dust accumulation anomaly on the Greenland summit,

https://doi.org/10.5194/cp-2022-89
Preprint. Discussion started: 28 November 2022


Climate of the Past Discussions

interpreted to represent a shift in atmospheric circulation from 6000-5100 YBP, may be related to these features (Mayewski et al., 2004). Consistent with the small magnitude of cen-mil variations in general (Fig. 3), interactions with other trends (Fig. 5), and the spatial variability of such dynamics (Fig. 6), the mid-Holocene anomaly does not appear in all records or regions (Wanner et al., 2008).

4.3 Potential drivers

The dynamics driving the two patterns of cen-mil variation here (broad-scale millennial variations including at 5600-4500 YBP and northeast coastal multi-century variations) need further investigation. As noted above, the north-south differences across mid-latitude ENA may indicate a role for variability in the Atlantic pressure gradient similar to the North Atlantic Oscillation at monthly to interannual time scales. NAO-like dynamics may be expressed at cen-mil scales (Olsen et al., 2012; Orme et al., 2021) and are usually strongest in winter, but they can have an important form of expression in summer, extending from North America to Europe (Folland et al., 2009). A weak latitudinal temperature gradient from 5600-4500 YBP followed by a steep gradient from 4500-3900 YBP (Fig. 6) could be consistent with negative and positive NAO phases. The prominence of the mid-Holocene shift in the ENA records examined here (Fig. 6-7) and elsewhere (Willard et al., 2005) also raises the question of whether the change originated from feedbacks that affect Atlantic sector pressure gradients such as by altering the depth of the African monsoon low (Claussen et al., 1999), potential via dust loading feedbacks (Pausata et al., 2016), or whether millennial-scale variation interfered with long trends to produce state-shifts on multiple continents at approximately the same time.

The multi-century variability expressed along the Atlantic coast has similarities to variations also observed in other Atlantic sectors, including off the west African coast (Adkins et al., 2006; deMenocal et al., 2000) and the Mediterranean (Fletcher et al., 2013). Holocene simulations indicate Atlantic-African-American linkages should be expected (Muschitiello et al., 2015). These sectors may be linked via the dynamics of the North Atlantic subtropical high (Clement et al., 2015), possibly driven by cloud feedbacks (Bellomo et al., 2016), atmospheric feedbacks on meridional overturning (Wills et al., 2019) or volcanism (Birkel et al., 2018; Kobashi et al., 2017); similar dynamics on interannual scales have consequences for North American hydroclimate patterns (Enfield et al., 2001; Anchukaitis et al., 2019).

A preliminary comparison of alkenone records from the Scotian and Virginia margins (Sachs, 2007) and the west African margin (Adkins et al., 2006) reveal that they potentially share a multi-century pattern of variability over the past 6000 years, which is expressed by different sign changes between Scotian and African margins with the sign of the variation switching between early and late events off Virginia (Fig. 8). Principal components analysis indicates that, at face value given current age control, the pattern represents 11% of the variance within the three records over the past 8000 years, but 23% in the past 6000 years. (The first PC represents 72% of the variance and the long-term trend over the past 8000 years, Fig. 2D). The multi-century SST variability correlates with the coastal hydroclimate variability (Fig. 8) and may also involve shifts in the

https://doi.org/10.5194/cp-2022-89
Preprint. Discussion started: 28 November 2022

Climate of the Past Discussions
Open Access
EGU

480 temperature gradient over the western Atlantic and Greenland (Shuman et al., 2019). However, the multi-century SST and hydroclimate variability along the western Atlantic margin does not extend to similar large-scale temperature gradient changes (Fig. 8). Therefore, at least two different dynamics, even if they are different seasonal expressions of NAO-like variations, must be involved.

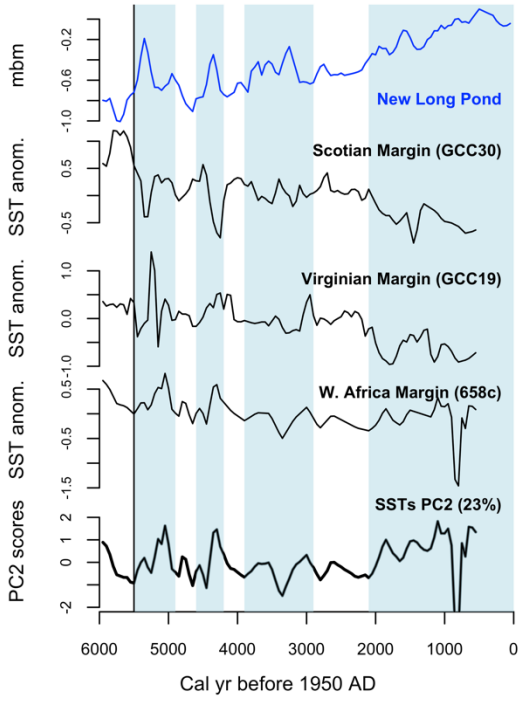

485

Figure 8. Comparison of the lake-level record from New Long Pond, Massachusetts (Fig. 2H), and three alkenone-inferred sea-surface temperature (SST) records (Adkins et al., 2006; Sachs, 2007). The SST records are shown after detrending and with the second principal component (PC2) scores of a PCA conducted on the non-detrended series; the first PC captures the trends. Blue bands represent the timing of wet phases identified from radiocarbon dated paleoshorelines at multiple lakes in coastal 490 **Massachusetts (Newby et al., 2014). "MBM" refers to meters below modern water level.**

4.4 Signal detection

Cen-mil variability is small relative to the ability to detect it. Several factors may aid efforts to examine these dynamics, however. First, analyses of calibrated rather than relative paleoclimate records may aid detection if all records record variations 495 in similar, linear ways. For example, calibration of fossil pollen using the modern analog or similar techniques removes inherent non-linearities in the responses of individual plant taxa and isolates the effects of focal climate variables from the interacting influences of other factors. While the responses of individual taxa are non-linear, the calibrated pollen assemblage (plant community) response is likely to be linear (Shuman et al., 2019). Other relative paleoclimate indices may be more

https://doi.org/10.5194/cp-2022-89
Preprint. Discussion started: 28 November 2022

complex (Axford et al., 2011), particularly if they are not multi-variate and only shift in a bivariate fashion with respect to a wide range of different influences (e.g., sediment carbon:nitrogen ratios, stable isotopes). Such data series may not be meaningfully different from random noise (Fig. 1A) in some settings if multiple competing influences interact to create complex signals.

Second, ensembles of detailed, well-dated records from the same climatic region or scale ensure that noise can be removed through averaging (Fig. 1). Third, comparisons of independent ensembles allow the signals to be cross validated. Analyses here benefitted from ensembles based on many cores (>600 fossil pollen records, >30 cores across nine lake-level study sites, dozens of marine records), which reduced age and reconstruction uncertainties. The different ensembles of temperature and moisture were also developed in fundamentally different ways (e.g., microfossil versus physical sedimentological analyses), which indicated that any shared signals had a broad basis of evidence indicating multivariate environmental responses to even weak climate fluctuations.

5 Conclusions

In areas centered on mid-latitude eastern North American, coherent cen-mil variation has similar signal magnitudes in independent temperature and hydroclimate datasets. The major signals, including prominent mid-Holocene anomalies from 5600-4500 YBP, are not readily falsified using the analyses here because they share the characteristics of non-random signals. The variations played important roles in mediating long-term trends, creating differences in the timing of the Holocene thermal maximum and rates of early-Holocene warming and late-Holocene cooling among regions. Events that have previously attracted focused attention, such as at 9300, 8200, 4200, and 2700 YBP, do not stand out as the most distinct features of the ensembles of data compiled here.

Instead, two major patterns of variability appear evident. One appears expressed across a broad range of spatial scales, which is similar to some unforced global variability in transient climate simulations (Marsicek et al., 2018; Wan et al., 2019). The pattern includes a set of millennia fluctuations with important anomalies and rapid shifts in both temperature and moisture gradients at ca. 5500 and 2100 YBP. More work is needed to evaluate whether such broad-scale changes, including the mid-Holocene anomaly, stem from external forcing, such as solar or volcanic events, intrinsic ocean or atmosphere variability, or other factors such as surface-atmosphere feedbacks, but the spatial patterns indicate that shifts in summer atmospheric pressure gradients over the Atlantic, such as associated with the NAO at short time scales, may be involved. The second major pattern produced a series of multi-century hydroclimate fluctuations along the Atlantic coast and may relate to Atlantic SST variability with distinctive spectral properties not seen in most of the study area. Because pollen and lake-level records detect the events, they had ecological, hydrological, geomorphic, and therefore, likely human significance and deserve further investigation.

https://doi.org/10.5194/cp-2022-89
Preprint. Discussion started: 28 November 2022

6 Data availability

The different ensembles of data examined here are available through the NOAA National Centers for Environmental Information Paleoclimatology Database:

- North Atlantic and adjacent continental reconstructions (Marsicek et al., 2018): https://www.ncdc.noaa.gov/paleo-search/study/22992
- ENA and sub-regional temperature and moisture reconstructions (Shuman and Marsicek, 2016): https://www.ncdc.noaa.gov/paleo-search/study/31097
- New Long Pond, Massachusetts, USA (coastal northeast U.S.) lake-level reconstruction (Newby et al., 2014): https://www.ncdc.noaa.gov/paleo-search/study/23074
- Scotian Margin sea-surface temperature reconstruction (OCE326-GGC30) (Sachs, 2007): https://www.ncdc.noaa.gov/paleo-search/study/6409

7 Acknowledgements

This work was supported by funding from U.S. National Science Foundation (DEB-1856047; EAR-1903729). C. Routson, C. Morrill, L. Curtin and D. Groff kindly provided thoughtful comments on the manuscript.

The author declares that he has no conflict of interest.

https://doi.org/10.5194/cp-2022-89
Preprint. Discussion started: 28 November 2022

8 References

Adkins, J., deMenocal, P., and Eshel, G.: The African humid period and the record of marine upwelling from excess 230Th in Ocean Drilling Program Hole 658C, Paleoceanography, 21, PA4203, https://doi.org/10.1029/2005pa001200, 2006.

Anchukaitis, K. J., Cook, E. R., Cook, B. I., Pearl, J., D'Arrigo, R., and Wilson, R.: Coupled Modes of North Atlantic Ocean-Atmosphere Variability and the Onset of the Little Ice Age, Geophys. Res. Lett., 46, 12417–12426, https://doi.org/10.1029/2019GL084350, 2019.

Ault, T. R., Cole, J. E., Overpeck, J. T., Pederson, G. T., George, S. S., Otto-Bliesner, B., Woodhouse, C. A., and Deser, C.: The Continuum of Hydroclimate Variability in Western North America during the Last Millennium, J. Clim., 26, 5863–5878, 2013.

Ault, T. R., George, S. S., Smerdon, J. E., Coats, S., Mankin, J. S., Carrillo, C. M., Cook, B. I., and Stevenson, S.: A Robust Null Hypothesis for the Potential Causes of Megadrought in Western North America, J. Clim., 31, 3–24, https://doi.org/10.1175/JCLI-D-17-0154.1, 2018.

Axford, Y., Andresen, C. S., Andrews, J. T., Belt, S. T., Geirsdóttir, Á., Massé, G., Miller, G. H., Ólafsdóttir, S., and Vare, L. L.: Do paleoclimate proxies agree? A test comparing 19 late Holocene climate and sea-ice reconstructions from Icelandic marine and lake sediments, J. Quat. Sci., 26, 645–656, https://doi.org/10.1002/jqs.1487, 2011.

Bellomo, K., Clement, A. C., Murphy, L. N., Polvani, L. M., and Cane, M. A.: New observational evidence for a positive cloud feedback that amplifies the Atlantic Multidecadal Oscillation, Geophys. Res. Lett., 43, 9852–9859, https://doi.org/10.1002/2016GL069961, 2016.

Bender, M. L.: Paleoclimate, 2013.

Benson, L., Kashgarian, M., Rye, R., Lund, S., Paillet, F., Smoot, J., Kester, C., Mensing, S., Meko, D., and Lindström, S.: Holocene multidecadal and multicentennial droughts affecting Northern California and Nevada, Quat. Sci. Rev., 21, 659–682, 2002.

Berger, A.: Long-term variations of caloric insolation resulting from the earth's orbital elements, Quat. Res., 9, 139–167, 1978.

Berke, M. A., Johnson, T. C., Werne, J. P., Schouten, S., and Sinninghe Damsté, J. S.: A mid-Holocene thermal maximum at the end of the African Humid Period, Earth Planet. Sci. Lett., 351–352, 95–104, https://doi.org/10.1016/j.epsl.2012.07.008, 2012.

Birkel, S. D., Mayewski, P. A., Maasch, K. A., Kurbatov, A. V., and Lyon, B.: Evidence for a volcanic underpinning of the Atlantic multidecadal oscillation, Npj Clim. Atmospheric Sci., 1, 1–7, https://doi.org/10.1038/s41612-018-0036-6, 2018.

https://doi.org/10.5194/cp-2022-89
Preprint. Discussion started: 28 November 2022

Cacho, I., Grimalt, J. O., Canals, M., Sbaffi, L., Shackleton, N. J., Schönfeld, J., and Zahn, R.: Variability of the western Mediterranean Sea surface temperature during the last 25,000 years and its connection with the Northern Hemisphere climatic changes, Paleoceanography, 16, 40–52, https://doi.org/10.1029/2000PA000502, 2001.

Camill, P., Umbanhowar Jr, C. E., Teed, R., Geiss, C. E., Aldinger, J., Dvorak, L., Kenning, J., Limmer, J., and Walkup, K.: Late-glacial and Holocene climatic effects on fire and vegetation dynamics at the prairie-forest ecotone in south-central Minnesota, J. Ecol., 91, 822–836, 2003.

Claussen, M., Kubatzki, C., Brovkin, V., Ganopolski, A., Hoelzmann, P., and Pachur, H. J.: Simulation of an abrupt change in Saharan vegetation in the mid-Holocene, Geophys. Res. Lett., 26, 2037–2040, 1999.

Clement, A., Bellomo, K., Murphy, L. N., Cane, M. A., Mauritsen, T., Rädel, G., and Stevens, B.: The Atlantic Multidecadal Oscillation without a role for ocean circulation, Science, 350, 320–324, https://doi.org/10.1126/science.aab3980, 2015.

Crucifix, M., de Vernal, A., Franzke, C., and von Gunten, L.: Centennial to Millennial Climate Variability, 131–166, https://doi.org/10.22498/pages.25.3, 2017.

Dean, W. E.: Rates, timing, and cyclicity of Holocene eolian activity in north-central United States; evidence from varved lake sediments, Geology, 25, 331–334, 1997.

deMenocal, P., Ortiz, J., Guilderson, T., and Sarnthein, M.: Coherent High- and Low-Latitude Climate Variability During the Holocene Warm Period, Science, 288, 2198–2202, https://doi.org/10.1126/science.288.5474.2198, 2000.

deMenocal, P. B.: Cultural Responses to Climate Change During the Late Holocene, Science, 292, 667–673, https://doi.org/10.1126/science.1059287, 2001.

Dyke, A. S.: An outline of North American deglaciation with emphasis on central and northern Canada, in: Developments in Quaternary Science, edited by: Ehlers, J. and Gibbard, P. L., Elsevier, 373–424, 2004.

Enfield, D. B., Mestas-Nuñez, A. M., and Trimble, P. J.: The Atlantic Multidecadal Oscillation and its relation to rainfall and river flows in the continental U.S., Geophys. Res. Lett., 28, 2077–2080, https://doi.org/10.1029/2000GL012745, 2001.

Fastovich, D., Russell, J. M., Jackson, S. T., Krause, T. R., Marcott, S. A., and Williams, J. W.: Spatial Fingerprint of Younger Dryas Cooling and Warming in Eastern North America, Geophys. Res. Lett., 47, e2020GL090031, https://doi.org/10.1029/2020GL090031, 2020.

https://doi.org/10.5194/cp-2022-89
Preprint. Discussion started: 28 November 2022

Fletcher, W. J., Debret, M., and Goñi, M. F. S.: Mid-Holocene emergence of a low-frequency millennial oscillation in western Mediterranean climate: Implications for past dynamics of the North Atlantic atmospheric westerlies, The Holocene, 23, 153–166, https://doi.org/10.1177/0959683612460783, 2013.

Folland, C. K., Knight, J., Linderholm, H. W., Fereday, D., Ineson, S., and Hurrell, J. W.: The Summer North Atlantic Oscillation: Past, Present, and Future, J. Clim., 22, 1082–1103, https://doi.org/10.1175/2008JCLI2459.1, 2009.

Giraudeau, J., Grelaud, M., Solignac, S., Andrews, J. T., Moros, M., and Jansen, E.: Millennial-scale variability in Atlantic water advection to the Nordic Seas derived from Holocene coccolith concentration records, Quat. Sci. Rev., 29, 1276–1287, https://doi.org/10.1016/j.quascirev.2010.02.014, 2010.

Grimm, E. C.: Trends and palaeoecological problems in the vegetation and climate history of the northern Great Plains, U.S.A, Biol. Environ. Proc. R. Ir. Acad., 99B, 1–18, 2001.

Hernández, A., Martin-Puertas, C., Moffa-Sánchez, P., Moreno-Chamarro, E., Ortega, P., Blockley, S., Cobb, K. M., Comas-Bru, L., Giralt, S., Goosse, H., Luterbacher, J., Martrat, B., Muscheler, R., Parnell, A., Pla-Rabes, S., Sjolte, J., Scaife, A. A., Swingedouw, D., Wise, E., and Xu, G.: Modes of climate variability: Synthesis and review of proxy-based reconstructions through the Holocene, Earth-Sci. Rev., 209, 103286, https://doi.org/10.1016/j.earscirev.2020.103286, 2020.

Hurrell, J. W., Kushnir, Y., Ottersen, G., and Visbeck, M.: The North Atlantic Oscillation, https://doi.org/10.1029/134GM01, 2003.

Huybers, P. and Curry, W.: Links between annual, Milankovitch and continuum temperature variability, Nature, 441, 329–332, https://doi.org/10.1038/nature04745, 2006.

Jackson, M. G., Oskarsson, N., Trønnes, R. G., McManus, J. F., Oppo, D. W., Grönvold, K., Hart, S. R., and Sachs, J. P.: Holocene loess deposition in Iceland: Evidence for millennial-scale atmosphere-ocean coupling in the North Atlantic, Geology, 33, 509–512, https://doi.org/10.1130/G21489.1, 2005.

Karnauskas, K. B., Smerdon, J. E., Seager, R., and González-Rouco, J. F.: A Pacific Centennial Oscillation Predicted by Coupled GCMs*, J. Clim., 25, 5943–5961, https://doi.org/10.1175/JCLI-D-11-00421.1, 2012.

Kobashi, T., Menviel, L., Jeltsch-Thömmes, A., Vinther, B. M., Box, J. E., Muscheler, R., Nakaegawa, T., Pfister, P. L., Döring, M., Leuenberger, M., Wanner, H., and Ohmura, A.: Volcanic influence on centennial to millennial Holocene Greenland temperature change, Sci. Rep., 7, 1441, https://doi.org/10.1038/s41598-017-01451-7, 2017.

Larsen, D. J., Miller, G. H., Geirsdóttir, Á., and Ólafsdóttir, S.: Non-linear Holocene climate evolution in the North Atlantic: a high-resolution, multi-proxy record of glacier activity and environmental

https://doi.org/10.5194/cp-2022-89
Preprint. Discussion started: 28 November 2022

change from Hvítárvatn, central Iceland, Quat. Sci. Rev., 39, 14–25, https://doi.org/10.1016/j.quascirev.2012.02.006, 2012.

Liu, Z., Zhu, J., Rosenthal, Y., Zhang, X., Otto-Bliesner, B. L., Timmermann, A., Smith, R. S., Lohmann, G., Zheng, W., and Timm, O. E.: The Holocene temperature conundrum, Proc. Natl. Acad. Sci., 111, E3501–E3505, https://doi.org/10.1073/pnas.1407229111, 2014.

Lochte, A. A., Schneider, R., Kienast, M., Repschläger, J., Blanz, T., Garbe-Schönberg, D., and Andersen, N.: Surface and subsurface Labrador Shelf water mass conditions during the last 6000 years, Clim. Past, 16, 1127–1143, https://doi.org/10.5194/cp-16-1127-2020, 2020.

Magny, M. and Haas, J. N.: A major widespread climatic change around 5300 cal. yr BP at the time of the Alpine Iceman, J. Quat. Sci., 19, 423–430, https://doi.org/10.1002/jqs.850, 2004.

Magny, M., Leuzinger, U., Bortenschlager, S., and Haas, J. N.: Tripartite climate reversal in Central Europe 5600-5300 years ago, Quat. Res., 65, 3–19, 2006.

Marcott, S. A., Shakun, J. D., Clark, P. U., and Mix, A. C.: A Reconstruction of Regional and Global Temperature for the Past 11,300 Years, Science, 339, 1198–1201, https://doi.org/10.1126/science.1228026, 2013.

Marsicek, J., Shuman, B. N., Bartlein, P. J., Shafer, S. L., and Brewer, S.: Reconciling divergent trends and millennial variations in Holocene temperatures, Nature, 554, 92–96, https://doi.org/10.1038/nature25464, 2018.

Marsicek, J. P., Shuman, B., Brewer, S., Foster, D. R., and Oswald, W. W.: Moisture and temperature changes associated with the mid-Holocene Tsuga decline in the northeastern United States, Quat. Sci. Rev., 80, 333–342, https://doi.org/10.1016/j.quascirev.2013.09.001, 2013.

Martínez-Sosa, P., Tierney, J. E., Stefanescu, I. C., Dearing Crampton-Flood, E., Shuman, B. N., and Routson, C.: A global Bayesian temperature calibration for lacustrine brGDGTs, Geochim. Cosmochim. Acta, 305, 87–105, https://doi.org/10.1016/j.gca.2021.04.038, 2021.

Mayewski, P. A., Rohling, E., Stager, C., Karlen, K., Maasch, K., Meeker, L. D., Meyerson, E., Gasse, F., van Kreveld, S., Holmgren, K., Lee-Thorp, J., Rosqvist, G., Rack, F., Staubwasser, M., and Shneider, R.: Holocene climate variability, Quat. Res., 62, 243, 2004.

Miao, X., Mason, J. A., Johnson, W. C., and Wang, H.: High-resolution proxy record of Holocene climate from a loess section in Southwestern Nebraska, USA, Palaeogeogr. Palaeoclimatol. Palaeoecol., 245, 368–381, https://doi.org/10.1016/j.palaeo.2006.09.004, 2007.

https://doi.org/10.5194/cp-2022-89
Preprint. Discussion started: 28 November 2022

Muschitiello, F., Zhang, Q., Sundqvist, H. S., Davies, F. J., and Renssen, H.: Arctic climate response to the termination of the African Humid Period, Quat. Sci. Rev., 125, 91–97, https://doi.org/10.1016/j.quascirev.2015.08.012, 2015.

Nelson, D. M. and Hu, F. S.: Patterns and drivers of Holocene vegetational change near the prairie-forest ecotone in Minnesota: revisiting McAndrews' transect, New Phytol., 179, 449–459, 2008.

Newby, P., Shuman, B., Donnelly, J. P., Karnauskas, K. B., and Marsicek, J. P.: Centennial-to-Millennial Hydrologic Trends and Variability along the North Atlantic Coast, U.S.A., during the Holocene, Geophys Res Lett, 41, https://doi.org/10.1002/2014GL060183, 2014.

Newby, P. E., Shuman, B. N., Donnelly, J. P., and MacDonald, D.: Repeated century-scale droughts over the past 13,000 yrs near the Hudson River watershed, USA, Quat. Res., 75, 523–530, 2011.

Olsen, J., Anderson, N. J., and Knudsen, M. F.: Variability of the North Atlantic Oscillation over the past 5,200 years, Nat. Geosci., 5, 808–812, https://doi.org/10.1038/ngeo1589, 2012.

Oppo, D. W., McManus, J. F., and Cullen, J. L.: Palaeo-oceanography: Deepwater variability in the Holocene epoch, Nature, 422, 277–277, 2003.

Orme, L. C., Miettinen, A., Seidenkrantz, M.-S., Tuominen, K., Pearce, C., Divine, D. V., Oksman, M., and Kuijpers, A.: Mid to late-Holocene sea-surface temperature variability off north-eastern Newfoundland and its linkage to the North Atlantic Oscillation, The Holocene, 31, 3–15, https://doi.org/10.1177/0959683620961488, 2021.

PAGES 2k Consortium: Continental-scale temperature variability during the past two millennia, Nat. Geosci., 6, 339–346, https://doi.org/10.1038/NGEO1797, 2013.

Pausata, F. S. R., Messori, G., and Zhang, Q.: Impacts of dust reduction on the northward expansion of the African monsoon during the Green Sahara period, Earth Planet. Sci. Lett., 434, 298–307, https://doi.org/10.1016/j.epsl.2015.11.049, 2016.

Percival, D. B., Walden, A. T., B, P. D., and T, W. A.: Spectral Analysis for Physical Applications, Cambridge University Press, 616 pp., 1993.

R Core Development Team: R: A language and environment for statistical computing., R Foundation for Statistical Computing, Vienna, Austria, 2020.

Renssen, H., Goosse, H., and Muscheler, R.: Coupled climate model simulation of Holocene cooling events: oceanic feedback amplifies solar forcing, Clim. Past, 2, 79–90, 2006.

Russell, J. M., Hopmans, E. C., Loomis, S. E., Liang, J., and Sinninghe Damsté, J. S.: Distributions of 5- and 6-methyl branched glycerol dialkyl glycerol tetraethers (brGDGTs) in East African lake

sediment: Effects of temperature, pH, and new lacustrine paleotemperature calibrations, Org. Geochem., 117, 56–69, https://doi.org/10.1016/j.orggeochem.2017.12.003, 2018.

Sachs, J. P.: Cooling of Northwest Atlantic slope waters during the Holocene, Geophys Res Lett, 34, L03609, https://doi.org/10.1029/2006gl028495, 2007.

Saltzman, B.: Stochastically-driven climatic fluctuations in the sea-ice, ocean temperature, CO2 feedback system, Tellus, 34, 97–112, https://doi.org/10.1111/j.2153-3490.1982.tb01797.x, 1982.

Schmidt, M. W., Weinlein, W. A., Marcantonio, F., and Lynch-Stieglitz, J.: Solar forcing of Florida Straits surface salinity during the early Holocene, Paleoceanography, 27, https://doi.org/10.1029/2012PA002284, 2012.

Shuman, B. N. and Burrell, S. A.: Centennial to millennial hydroclimatic fluctuations in the humid northeast United States during the Holocene, Quat. Res., 1–11, https://doi.org/10.1017/qua.2017.62, 2017.

Shuman, B. N. and Marsicek, J. P.: The Structure of Holocene Climate Change in Mid-Latitude North America, Quat. Sci. Rev., 141, 38–51, 2016.

Shuman, B. N., Carter, G. E., Hougardy, D. D., Powers, K., and Shinker, J. J.: A north–south moisture dipole at multi century scales in the Central and Southern Rocky Mountains during the late Holocene, Rocky Mt. Geol., 49, 17–33, 2014.

Shuman, B. N., Marsicek, J., Oswald, W. W., and Foster, D. R.: Predictable hydrological and ecological responses to Holocene North Atlantic variability, Proc. Natl. Acad. Sci., 116, 5985–5990, https://doi.org/10.1073/pnas.1814307116, 2019.

Slutzky, E.: The Summation of Random Causes as the Source of Cyclic Processes, Econometrica, 5, 105–146, https://doi.org/10.2307/1907241, 1937.

Telford, R. J. and Birks, H. J. B.: A novel method for assessing the statistical significance of quantitative reconstructions inferred from biotic assemblages, Quat. Sci. Rev., 30, 1272–1278, https://doi.org/10.1016/j.quascirev.2011.03.002, 2011.

Thompson, L. G., Mosley-Thompson, E., Davis, M. E., Henderson, K. A., Brecher, H. H., Zagorodnov, V. S., Mashiotta, T. A., Lin, P.-N., Mikhalenko, V. N., Hardy, D. R., and Beer, J.: Kilimanjaro Ice Core Records: Evidence of Holocene Climate Change in Tropical Africa, Science, 298, 589–593, https://doi.org/10.1126/science.1073198, 2002.

Thornalley, D. J. R., Elderfield, H., and McCave, I. N.: Holocene oscillations in temperature and salinity of the surface subpolar North Atlantic, Nature, 457, 711–714, 2009.

https://doi.org/10.5194/cp-2022-89
Preprint. Discussion started: 28 November 2022

Wan, L., Liu, Z., Liu, J., Sun, W., and Liu, B.: Holocene temperature response to external forcing: assessing the linear response and its spatial and temporal dependence, Clim. Past, 15, 1411–1425, https://doi.org/10.5194/cp-15-1411-2019, 2019.

Wanner, H., Beer, J., Bütikofer, J., Crowley, T. J., Cubasch, U., Flückiger, J., Goosse, H., Grosjean, M., Joos, F., Kaplan, J. O., Küttel, M., Müller, S. A., Prentice, I. C., Solomina, O., Stocker, T. F., Tarasov, P., Wagner, M., and Widmann, M.: Mid- to Late Holocene climate change: an overview, Quat. Sci. Rev., 27, 1791–1828, 2008.

Willard, D. A., Bernhardt, C. E., Korejwo, D. A., and Meyers, S. R.: Impact of millennial-scale Holocene climate variability on eastern North American terrestrial ecosystems: pollen-based climatic reconstruction, Glob. Planet. Change, 47, 17–35, https://doi.org/10.1016/j.gloplacha.2004.11.017, 2005.

Williams, J. W. and Shuman, B.: Obtaining accurate and precise environmental reconstructions from the modern analog technique and North American surface pollen dataset, Quat. Sci. Rev., 27, 669–687, 2008.

Wills, R. C. J., Armour, K. C., Battisti, D. S., and Hartmann, D. L.: Ocean–Atmosphere Dynamical Coupling Fundamental to the Atlantic Multidecadal Oscillation, J. Clim., 32, 251–272, https://doi.org/10.1175/JCLI-D-18-0269.1, 2019.

.